



## Numerical Investigation of PV/T System Cooling Using Nanofluids

Khalid Salih Hamoudah <sup>1\*</sup>, Saleh Etaig <sup>2</sup>

<sup>1</sup> Department of Renewable Energy Engineering, Faculty of Engineering, Libyan Academy, Benghazi Branch, Benghazi, Libya.

<sup>2</sup> Mechanical Engineering Department, University of Benghazi, Benghazi, Libya

### دراسة رقمية عن منظومة تبريد ألواح كهروضوئية باستخدام موائع موائع النانو

خالد صالح حموده <sup>1\*</sup>، صالح عتيق <sup>2</sup>  
<sup>1</sup> قسم هندسة الطاقات المتجددة، الأكاديمية الليبية فرع بنغازي، بنغازي، ليبيا  
<sup>2</sup> قسم الهندسة الميكانيكية، جامعة بنغازي، بنغازي، ليبيا

\*Corresponding author: [khalidsalih2010@yahoo.com](mailto:khalidsalih2010@yahoo.com)

Received: March 01, 2024

Accepted: May 05, 2024

Published: May 30, 2024

#### Abstract:

A Photovoltaic/thermal system (PV/T) was devised and implemented to investigate enhancements in thermal and electrical efficiency through the utilization of nanofluids as coolants. The electrical efficiency witnessed a decline due to a notable reduction in the maximum power output of the photovoltaic cell as temperature increased. Consequently, this elongated the payback period of the PV system and potentially shortened the lifespan of the PV cell. To address this issue, an effective cooling technique was employed. The PV/T system incorporated a parallel plate thermal collector directly attached to the backside of the PV module using thermal paste. The cooling mechanism involved the use of (Al<sub>2</sub>O<sub>3</sub>-water) nanofluid with varying concentration ratios to mitigate the operating temperature. An elevation head of (Al<sub>2</sub>O<sub>3</sub>-water) was employed for passive cooling of the PV module. Numerical evaluation of the PV/T system's performance was conducted for different coolant concentrations, employing a 3D numerical analysis with finite element-based software Ansys. Under the influence of nanofluid at various concentration ratios (1-5%vol) at a constant inlet velocity (0.0001 m/s), the outlet temperature significantly increased to 76.6°C, while the PV cell temperature dropped to 51°C at a concentration ratio of 5%. This resulted in an improvement in the electrical efficiency of the solar panel to 12.69% and an increase in the thermal efficiency to 47.6%. The heat extracted from the PV module by the cooling nanofluid contributed to the overall energy output of the system.

**Keywords:** Photovoltaic/thermal (PV/T) hybrid system, Cooling, Nanofluids, thermal efficiency, Electrical efficiency.

#### المخلص

تم دراسة نظام الخلايا الكهروضوئية الحرارية لاختبار الكفاءة الحرارية والكهربائية باستخدام السوائل النانوية كسوائل تبريد. شهدت الكفاءة الكهربائية انخفاضاً بسبب الانخفاض الكبير في القدرة الكهربائية القصوى للخلية الكهروضوئية مع زيادة الحرارة، ولهذا السبب تم تمديد فترة استرداد نظام الطاقة الكهروضوئية وربما اختصار عمر الخلية الكهروضوئية. ولحل هذه المشكلة، يمكن استخدام تقنية التبريد بفعالية. نظام PV/T يتألف من مجمع حراري ذو لوحة موازية تم تثبيتها مباشرة على الجهة الخلفية للوحة الكهروضوئية باستخدام معجون حراري فقط، وكان تبريده يتم باستخدام سائل تبريد نانو مكون من (Al<sub>2</sub>O<sub>3</sub>) وماء (بتركيز مختلفة لتقليل درجة الحرارة التشغيلية). تم استخدام الانسياب الطبيعي لمائع التبريد اعتماداً على الارتفاع لتحقيق التبريد السلبي للوحة الكهروضوئية. تم تقييم أداء نظام PV/T عددياً لتركيز مختلفة من سائل التبريد، باستخدام تحليل رقمي ثلاثي الأبعاد باستخدام برنامج Ansys القائم على طريقة العناصر المحددة. تحت تأثير السائل النانوي بتركيز مختلفة (1-5% حجم) عند سرعة دخول ثابتة (0.0001 م/ث)، زادت درجة حرارة المخرج بشكل ملحوظ إلى 76.6 درجة مئوية، في حين انخفضت درجة حرارة الخلية الفوتوفولتائية إلى 51 درجة مئوية عند نسبة تركيز 5%. وأدى

ذلك إلى تحسين الكفاءة الكهربائية للوح الشمسي إلى 12.69% وزيادة الكفاءة الحرارية إلى 47.6%. الحرارة التي تم استخراجها من وحدة الفوتوفولتائية بواسطة السائل التبريدي النانوي ساهمت في الطاقة الإجمالية المنبعثة من النظام.

**الكلمات المفتاحية:** الأنظمة الكهروضوئية الحرارية الهجينة ، تبريد، موائع النانو، الكفاءة الحرارية ، الكفاءة الكهربائية

### Introduction:

The photovoltaic conversion efficiency is a measure of a solar cell's capability to convert incident solar radiation into usable electrical energy. Various factors, primarily irradiance and spectral distribution, influence this efficiency. Standard test conditions (STC), with 1000 W/m<sup>2</sup> irradiance, 25°C cell temperature, and AM1.5 spectrum, provide a benchmark for comparing cell performance.

However, there exists a theoretical maximum efficiency due to inherent physical limitations, particularly in crystalline silicon, where this limit is approximately 28% owing to three key factors [1]:

- Indirect Semiconductor Behavior: Silicon's indirect bandgap necessitates simultaneous photon and phonon (lattice vibration) absorption, resulting in lower intrinsic absorption compared to direct bandgap materials.
- Bandgap Energy: Only photons with energy surpassing the bandgap (1.1 eV for silicon) contribute to electricity generation. Others either pass through (transmission) or generate heat (non-radiative recombination), defining the cell's spectral response.
- Open-Circuit Voltage (Voc): Voc relies on carrier concentration and bandgap, typically reaching around 0.7 V for silicon.

Practical efficiency faces additional reduction due to several loss mechanisms:

- Optical Losses: These include reflection from the cell surface, shadowing by electrodes, and transmitted unabsorbed light.
- Ohmic Losses: Internal resistance from metal contacts, sheet resistance in doped layers, and leakage currents contribute to this type of loss.
- Recombination Losses: Photogenerated electrons and holes are lost before reaching the electrodes, mainly due to defect sites and impurities.

Comprehending these efficiency limitations and loss mechanisms is vital for advancing solar cell research and development, aiming for higher photovoltaic conversion efficiencies and fostering clean energy generation.

The current advancements in hybrid PV/T collectors have primarily focused on enhancing both electrical and thermal performances. Numerous research studies have explored the use of efficient nanofluids in solar technologies, introducing the concept of Nanofluids-based PVT systems [2, 3].

When compared to conventional solid-liquid suspensions for heat transfer intensification, properly engineered thermal nanofluids offer several advantages [4]:

- High dispersion stability with predominant Brownian motion of particles.
- High specific surface area and therefore more heat transfer surface between particles and fluids
- reduced pumping power as compared to pure liquid to achieve equivalent heat transfer intensification.
- reduced particle clogging as compared to conventional slurries, thus promoting system miniaturization.
- Adjustable properties, including thermal conductivity and surface wet ability, by varying particle concentrations to suit different applications.

### Literature Review

Numerous researchers have concentrated on utilizing various types of nanoparticles, including metals and metal oxides, to enhance the performance of Photovoltaic/Thermal (PV/T) systems. Various studies have explored the use of different nanofluids, consisting of base fluids with varying concentrations of nanoparticles, to improve the electrical and thermal efficiency of PV/T systems.

Considerations such as the type of nanomaterial, particle size, shape, and concentration play crucial roles in the effective design of nanofluid-based PV/T systems. Lelea et al. [5] examined the impact of cooling a concentrated PV/T system with Al<sub>2</sub>O<sub>3</sub> nanofluid, observing a decrease in module temperature compared to water cooling. Al-Waeli et al. [38] conducted an experimental study, finding that SiC cooling increased electrical, thermal, and overall efficiencies significantly compared to water cooling.

Xu and Kleinstreuer [6] suggested silicon-based nanofluid for domestic PV/T applications, citing an electrical efficiency of up to 11% and thermal efficiency reaching 59%. Khanjari et al. [7] used Computational Fluid Dynamics (CFD) to simulate PV/T collectors employing nanofluids, emphasizing the impact of nanoparticle volumetric ratio and heat transfer coefficient on efficiency.

Khanjari et al. [8] asserted that an increase in fluid inlet velocity led to a decrease in outlet fluid temperature, with a higher rate observed for Alumina-water nanofluids compared to Ag-water nanofluids. They claimed that an increase in fluid velocity resulted in decreased electrical efficiency and increased thermal efficiency, leading to an overall decrease in energy efficiency. Furthermore, they noted that electrical, thermal, and overall energy efficiencies increased with an increase in volume fraction.

Chandrasekar et al. [9] experimented with cooling a flat plate PV module using different nanofluids, reporting a decrease in cell temperature and an increase in electrical efficiency. Soltani Soltani et al. [10] tested various cooling methods for PV modules, highlighting the efficiency improvement with SiO<sub>2</sub>-water and Fe<sub>3</sub>O<sub>4</sub>-water nanofluid cooling.

Hussien et al. [11] demonstrated improved thermal and electrical efficiency in a PV/T system using Al<sub>2</sub>O<sub>3</sub>-water nanofluid as a coolant. Ebaid et al. [12] compared TiO<sub>2</sub>-water-polyethylene glycol and Al<sub>2</sub>O<sub>3</sub>-water-cetyltrimethylammonium bromide nanofluids, noting significant temperature reductions and efficiency improvements with nanofluid cooling.

Sardarabadi et al. [13] conducted experiments with Boehmite-based nanofluid cooling, achieving a substantial increase in electrical efficiency. Gangadevi et al. [14] observed increased electrical, thermal, and overall efficiencies in PV modules cooled with Al<sub>2</sub>O<sub>3</sub>-water nanofluid. Mustafa et al. [15] numerically investigated the influence of mass flow rate and nanofluid concentration (TiO<sub>2</sub>-water) on PV/T system efficiency, noting a linear relationship between electrical and thermal efficiency.

## Methodology

### • Numerical Method

The process of finding a numerical solution to complex physical problems, particularly in fluid dynamics, is known as Computational Fluid Dynamics (CFD). CFD software is employed to analyze these intricate physical processes, providing a more efficient and less time-consuming alternative to experimental setups. CFD allows for a comprehensive examination of fluid flow, considering its various physical properties simultaneously [16].

The analysis involves three primary equations that describe the relationships among the physical properties of interest. The formulation of these mathematical models depends on the specific physical situation under consideration, whether it involves heat transfer, mass transfer, phase transfer, etc. Validating the model against theoretical or experimental data is crucial for obtaining accurate solutions. In this study, the numerical analysis utilized ANSYS 2018 academic software.

### • Governing Equations of CFD

The governing equations used in computational fluid dynamics are derived from the three fundamental laws of conservation, emphasizing that mass, momentum, and energy are preserved within a closed system [16, 17]:

- 1- Conservation of Mass - expressed by the continuity equation.
- 2- Conservation of Momentum - based on Newton's second law.
- 3- Conservation of Energy - derived from the first law of thermodynamics.

These equations, representing the fundamental principles of fluid dynamics, work together to ensure that mass, momentum, and energy remain constant in the analyzed system.

To obtain a comprehensive understanding of the physical flow, the variables of velocity, pressure, and temperature must be determined simultaneously through these conservation equations. Pressure and temperature serve as the two independent thermodynamic variables required for this analysis. The resulting conservation equations also incorporate key thermodynamic properties such as density ( $\rho$ ), enthalpy ( $h$ ), viscosity ( $\mu$ ), and thermal conductivity ( $k$ ), which are determined based on the independent values of pressure and temperature. In any fluid flow scenario, it is essential to analyze velocity, pressure, and temperature at every point in the flow [18].

In the solid domains of the PV/T collector, heat transfer is predominantly studied through conduction. Conduction represents the mechanism by which thermal energy is transferred through the body via the vibration of particles. The heat transfer through the PV cell surface to the flow channel is addressed using the heat conduction equation.

$$\nabla \cdot (k \nabla T) = 0 \quad (1)$$

In the fluid domain within the flow collector channel, the heat transfer mechanism has been investigated as a conjugate heat transfer involving both conduction and convection. The equation governing conjugate heat transfer in the fluid domain, considering nanofluid as the working fluid, is expressed in this equation.

$$\rho C_p \frac{\partial T}{\partial t} + \rho C_p \cdot u \cdot \nabla T = \nabla \cdot (k \nabla T) + Q \quad (2)$$

The mass and momentum conservations for the fluid flow are given by this equation

$$\rho \frac{\partial u}{\partial t} + \nabla (\rho u) = 0 \quad (3)$$

$$\rho \frac{\partial u}{\partial t} + \rho (u \cdot \nabla) u = \nabla \cdot \left[ -\rho I + \mu (\nabla u + (\nabla u)^T) - \frac{2}{3} \mu (\nabla \cdot u) I \right] + F \quad (4)$$

Numerical simulations remain the most suitable approach for analyzing the thermal characteristics of PV/T collectors. The calculation of 3D temperature distributions involves the following assumptions:

- 1- The transmissivity of ethyl vinyl acetate (EVA) is approximately 100%.
- 2- The solar energy absorptivity is not affected by any dust on the surface.
- 3- The flow is steady, fully laminar, and incompressible.
- 4- Temperature variation along the thickness is considered negligible.
- 5- The thermal-physical properties of the absorber duct are assumed to be constant concerning the operating temperature.
- 6- The bottom side of the absorber duct is considered adiabatic.

• **PV/T Flat Plate Solar Collector Geometry**

Numerical simulations were conducted to assess the performance of the PV/T module. The analysis considered various parameters, including an inlet velocity of 0.0001 m/s, irradiation of 1000 W/m<sup>2</sup>, inlet temperature at 35°C, and ambient temperature at 35°C. The model comprised five solid domains for the PV module: front cover (glass), encapsulation (ethyl vinyl acetate (EVA)), PV cells, back sheet (tedlar), and thermal paste (as a heat conductor). The flow channel was composed of two domains: a solid domain (made of aluminum) and a fluid domain (water and water + Al<sub>2</sub>O<sub>3</sub>). The cross section of the PV/T model is illustrated in Figures 1 and 2. In total, the panel comprised nine layers, encompassing both solid and liquid layers, for the PV/T module. The simulations were performed using ANSYS Fluent software, solving the governing equations in a 3D steady-state condition. Data on the average cell surface temperature and average outlet temperature were extracted from the software, and corresponding graphs are presented

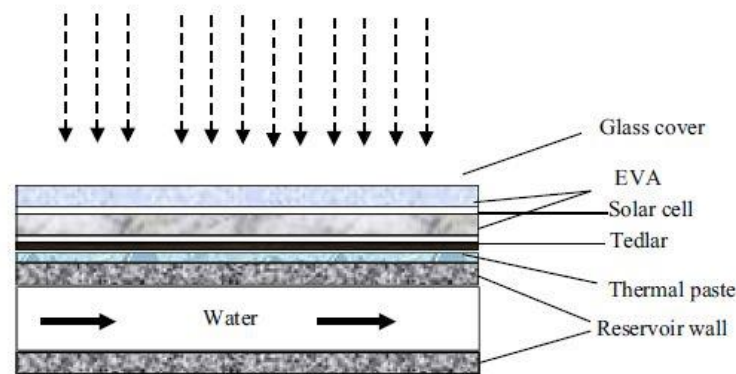


**Figure 1:** Cross sectional view of PV/T flat plate solar collector.

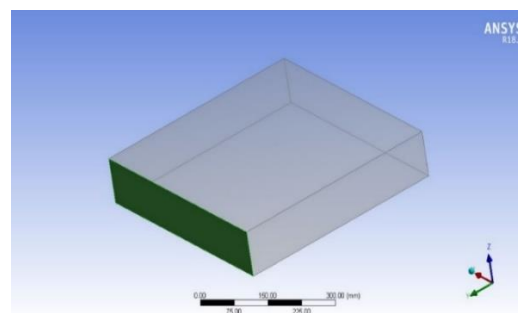


**Figure 2:** PV/T system geometry.

- **Boundary Conditions**

The computational domain was equipped with appropriate boundary conditions in accordance with the physics of the problem. The corresponding boundary conditions were applied to the heat transfer equations for the top (as external heat flux) and bottom layers of the PV module, as expressed by the following equation [19]:

$$-n \cdot q = h_c (T_{amb} - T_s) \quad (5)$$

In the provided equation,  $n$  where represents the surface normal, and  $T_s$  and  $T_{amb}$  denote the surface and ambient temperatures, the fluid domain featured specified inlet boundary conditions. These conditions were defined as a velocity inlet along the x-axis and an inlet water temperature, expressed by the following conditions

$$u = U_o, v = w = 0 \quad (6)$$

$$T_o = T_{in} \quad (7)$$

Wall boundary conditions were implemented to confine the fluid and solid regions, with the wall set at a no-slip condition. The outlet condition was maintained at zero-gauge pressure, and no viscous stress was applied.

$$\left[ \mu (\nabla u + (\nabla u)^T - \frac{2}{3} \mu (\nabla \cdot u) I \right] \cdot n = 0 \quad (\text{no slip condition}) \quad (8)$$

Thermal insulation is taken

$$-n \cdot (-k \nabla T) = 0 \quad (9)$$

The interface between the water and the absorber duct was designated as a wall with a coupled condition to facilitate conjugate heat transfer from the absorber duct to the water. An outflow boundary condition was applied at the outlet.

- **Mesh Generation**

In the present simulation software, mesh generation is the technique employed to subdivide a domain into a set of subdomains. The PV/T module was meshed using the physics-controlled mesh sequence setting available in the meshing setup, as illustrated in Figure 3. The number of mesh elements increases at each boundary to ensure accurate resolution of the heat transfer and flow fields.

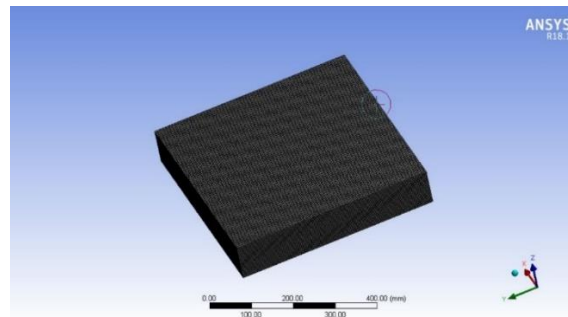


**Figure 3:** Mesh generation.

- **Mesh Independence test**

The CFD software divides the domain into numerous small subdomains known as cells, collectively forming the mesh, in order to attain a precise solution for the physical problem. Essentially, the domain of interest undergoes discretization into these small cells, allowing the application of mathematical equations under the assumption of linear behavior within each cell. Consequently, in regions where a parameter exhibits high sensitivity, a finer mesh is essential. It's noteworthy that the mesh often contributes to errors in the computed solution. In cases where the mesh lacks refinement in areas with highly fluctuating parameters, there is a heightened risk of obtaining results deviating significantly from reality.

To identify the most suitable mesh for the given physical problem, a mesh independence test is imperative. This test aims to strike a balance between achieving a competitive simulation runtime and obtaining the most accurate results. In this context, a mesh independence study was conducted to explore which type of mesh yields results closest to the theoretical value for the geometry. The study involved varying the element size, number of nodes, and number of elements one at a time.

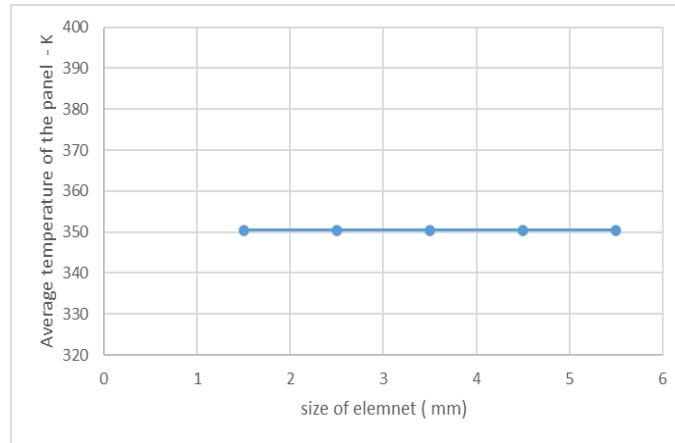


**Figure 4:** Mesh independence test.

- **Model Validation**

In this investigation, the CFD model was validated using air coolant fluid in a PV/T flat plate collector with eight cases. These cases encompassed various heat flux irradiance conditions and operational scenarios of the PV/T flat plate collector. The selected cases were run under steady-state conditions, assuming a controlled volume for simulation. The inlet velocity was held constant at 1.5 m/s, and the inlet temperature was set at 25°C. Solar radiation, with a normal component, was applied to the outer surface of the panel, and the heat flux was varied within the range of 200–1000 W/m<sup>2</sup>.

The surface wall temperature, calculated using the proposed CFD model, exhibited a high level of agreement with the experimental data obtained by Hasan et al. [20], as outlined in the table:

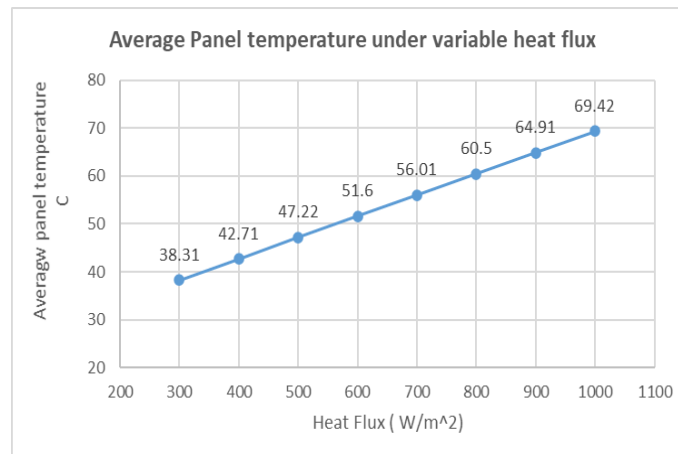


**Figure 5:** Validation of the CFD results with experimental data.

## Discussion

- **Effect of Nanofluid Concentrations on Outlet Temperature**

In Figure 6, the outlet temperature is depicted to decrease with an increase in nanofluid concentration until reaching a 3% volume concentration of nanofluid. Beyond this concentration, the outlet temperature shows an upward trend with an increase in nanofluid concentration. The mathematical relationship between the outlet temperature ( $T_c$ ) and the nanofluid concentration ( $\phi$ ) can be expressed by the following equation:

$$T_c = -0.0003\phi^4 + 0.0043\phi^3 - 0.0158\phi^2 + 0.0148\phi + 324.1$$

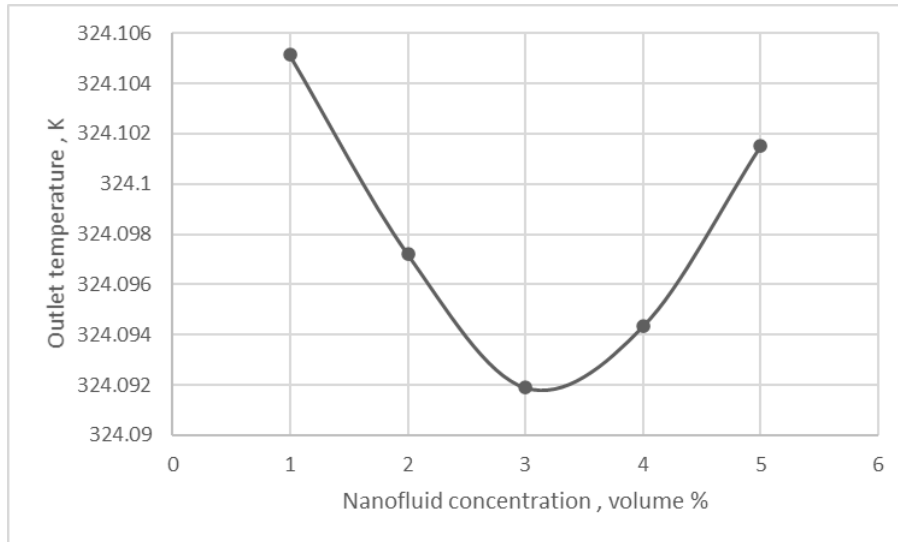


**Figure 6:** Effect of Nanofluid concentrations on an outlet temperature.

- **Effect of Nanofluid Concentrations on The PV Cell Temperature**

Figure 7, displays a PV cell temperature decreases with increases nanofluid concentrations, compared by water as coolant nanofluid is more active to remove PV Cell temperature.

The mathematical relationship between the PV cell temperature ( $T_w$ ) and nanofluid concentration ( $\emptyset$ ) is expressed by the following equation:  $T_w = 0.0104\emptyset^2 - 1.0185\emptyset + 354.44$

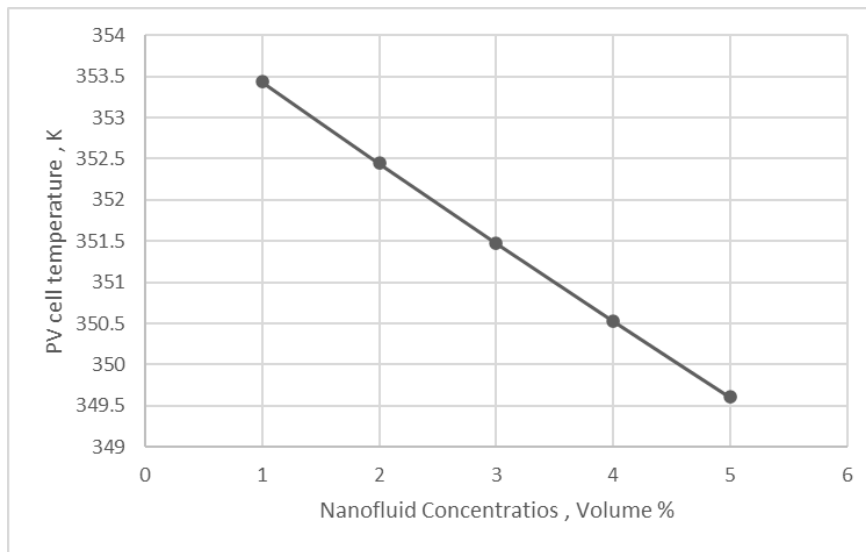


**Figure 7:** Effect of nanofluid concentrations on the PV cell Temperature.

- **Effect of Nanofluid Concentrations on a PV Cell Electrical Efficiency**

Figure 8, displays a PV cell electrical efficiency increases with increase nano fluid concentrations. The mathematical relationship between PV cell electrical efficiency ( $E_{cl}\%$ ) and nanofluid concentration ( $\emptyset$ ) can be expressed by the following equation:

$$E_{cl} \% = -6E-05 \emptyset^2 + 0.006 \emptyset + 12.67$$

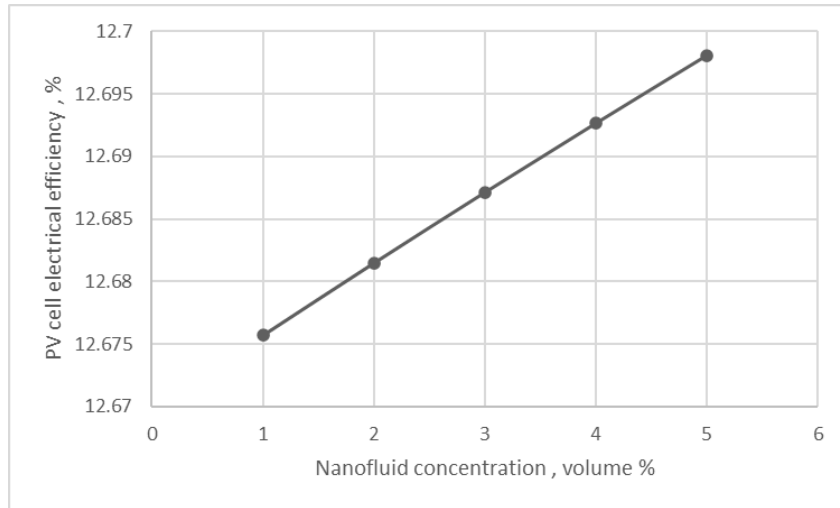


**Figure 8:** Effect of nanofluid concentrations on a PV cell's electrical efficiency.

- **Effect of Nanofluid Concentrations on A PV Cell Thermal Energy Efficiency**

In Figure 9, an increase in PV cell thermal energy efficiency is illustrated with an elevation in nanofluid concentrations. The mathematical relationship between PV cell thermal energy efficiency ( $E_{th}$  %) and nanofluid concentration ( $\emptyset$ ) can be expressed by the following equation:

$$E_{th} \% = -0.0099 \emptyset^2 + 0.9647 \emptyset + 43.072$$

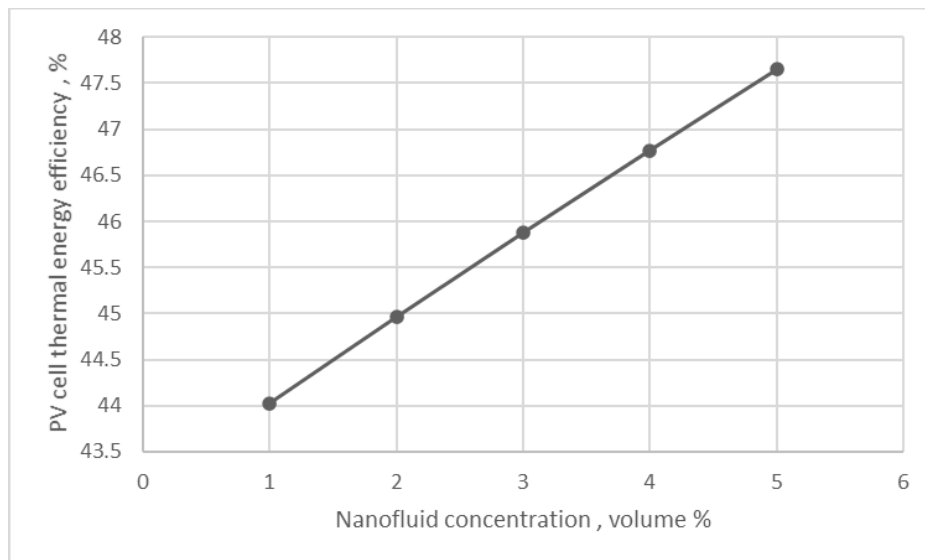


**Figure 9:** Effect of nanofluid concentrations on a PV cell thermal energy efficiency.

- **Effect of Nanofluid Concentrations on A Prandtl Number**

In Figure 10, it is illustrated that the Prandtl number increases with an elevation in nanofluid concentrations. The mathematical relationship between the Prandtl number ( $P_r$ ) and nanofluid concentration ( $\emptyset$ ) can be expressed by the following equation:

$$P_r = 0.0571 \emptyset^2 + 0.2714 \emptyset + 6.96$$



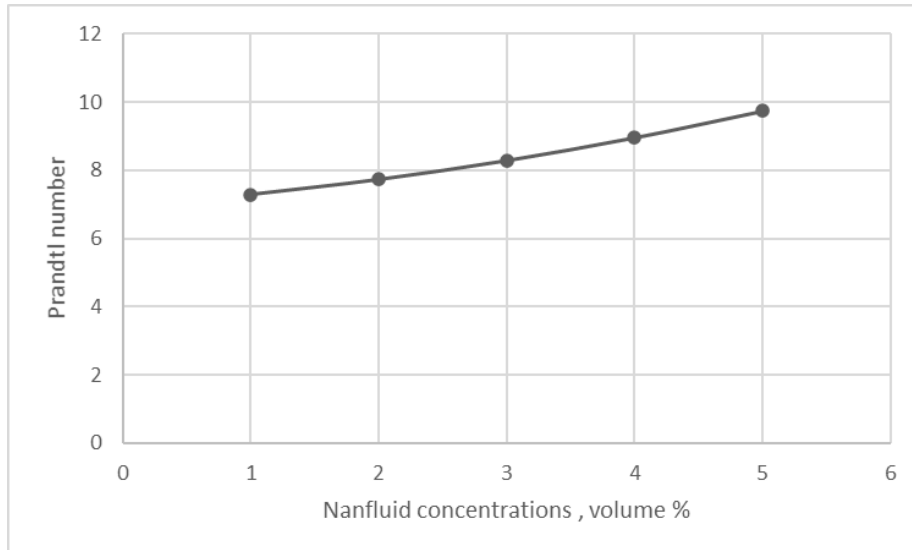


**Figure 10:** Effect of nanofluid concentrations on a Prandtl number.

- **Effect of Irradiation and Inlet Temperature on a PV Cell Outlet Temperature While Using Nonfluid and Water as Coolant**

Figures 11, 12, and 13, clarify that the outlet temperature of a PV cell remains nearly unchanged when nanofluids are utilized, as compared to using pure water as a coolant.

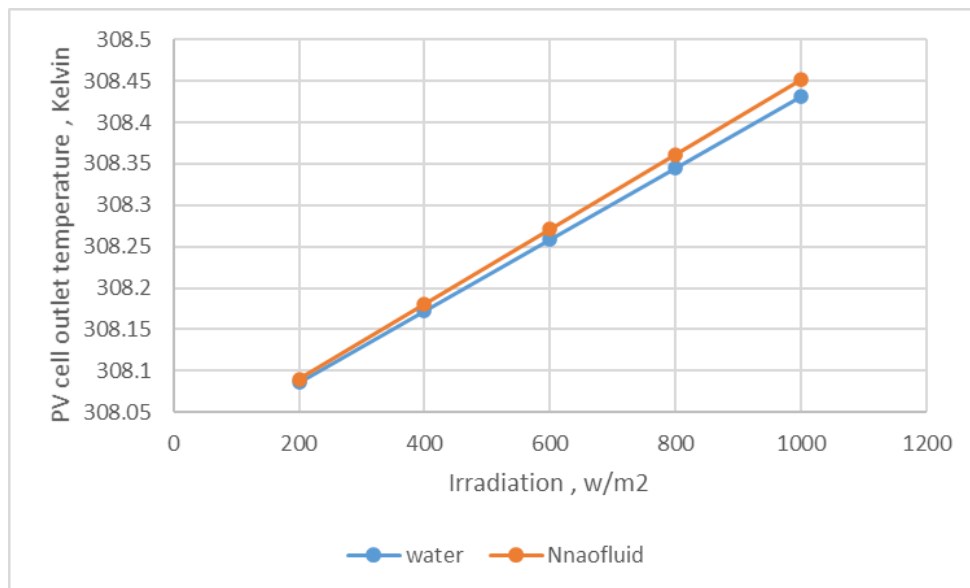


**Figure 11:** Effect of nanofluid inlet velocity on a PV cell outlet temperature  
 $v = 0.01$  m/sec,  $\phi = 5\%$ , inlet temperature = 308 K

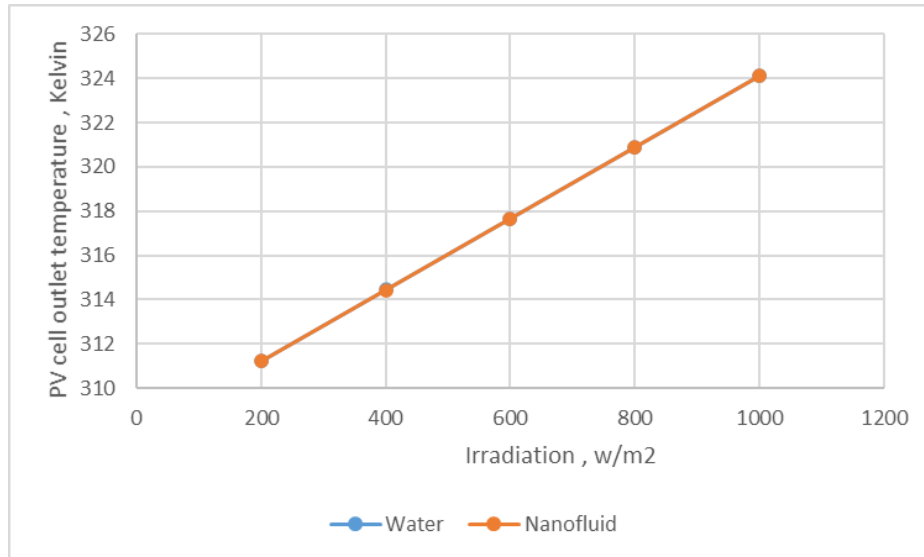


**Figure 12:** Effect of nanofluid inlet velocity on a PV cell outlet temperature  
 $v = 0.0001$  m/sec,  $\phi = 5\%$ , inlet temperature = 308 K

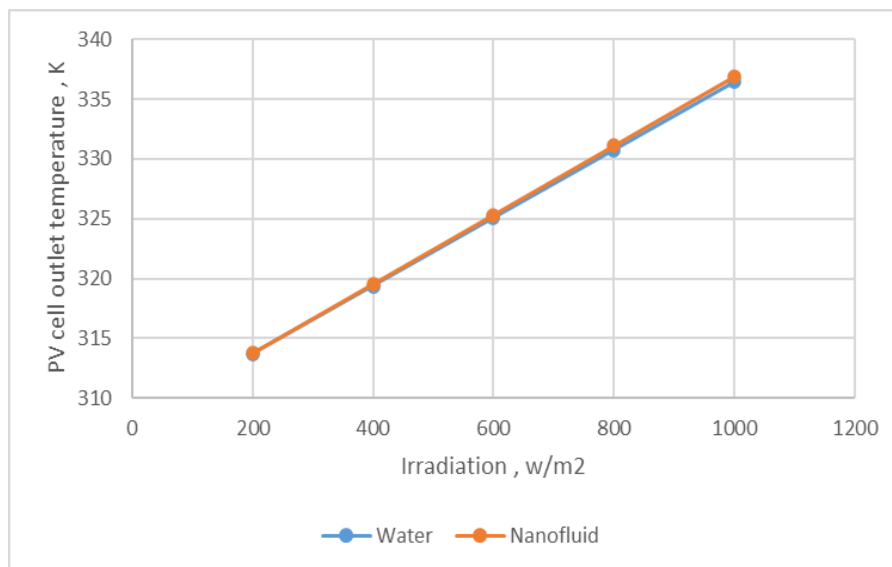


**Figure 13:** Effect of nanofluid inlet velocity on a PV cell outlet temperature  
 $v = 0.00005$  m/sec,  $\phi = 5\%$ , inlet temperature = 308 K

- **Effect of Nanofluid Concentrations on The Fill Factor**

Figure 14, demonstrates that the fill factor remains constant as the concentration of nanofluid increases. The mathematical relationship between the Fill Factor (FF) and nanofluid concentration ( $\phi$ ) can be expressed by the following equation:

$$FF = 0.0003 \phi^2 - 0.0045 \phi + 0.8408$$

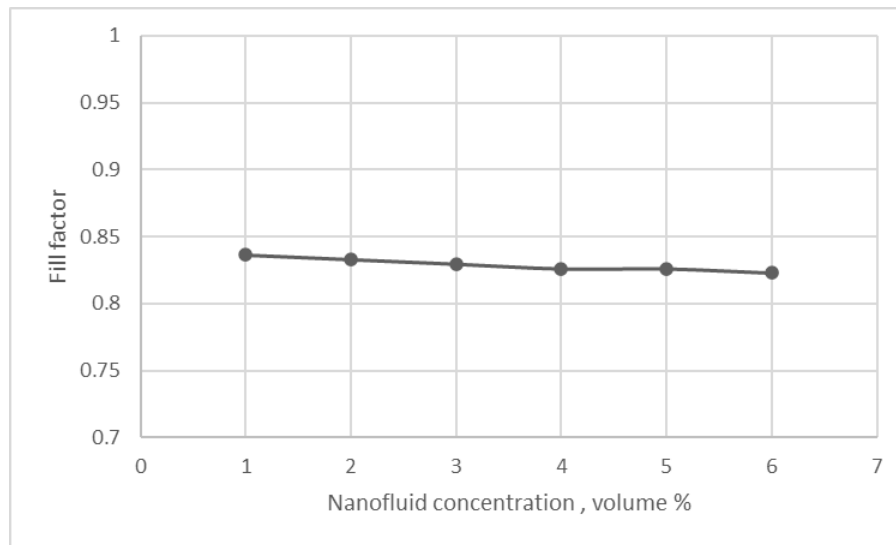


**Figure 14:** Effect of nanofluid concentrations on a Fill factor.

### Conclusion

This study investigated the impact of varying concentrations of ( $Al_2O_3$ ) nanofluid mixed with water on the performance of a PV/T flat-plate solar collector. The investigation considered different nanofluid concentrations, inlet velocities, solar irradiance levels, and constant ambient and inlet temperatures. Various parameters, including PV cell surface temperature, outlet temperature, electrical efficiency, thermal efficiency, overall efficiency, enhancement efficiency, and Prandtl number, were analyzed.

- Investigation of ( $Al_2O_3$ ) nanofluid concentrations in a PV/T flat-plate solar collector.
- Analysis of parameters including PV cell surface temperature, outlet temperature, electrical efficiency, thermal efficiency, overall efficiency, enhancement efficiency, and Prandtl number.
- Comparison of PV/T collector performance using nanofluid versus water as a base fluid coolant.
- At 5% nanofluid concentration, PV cell surface temperature decreased to 349.6 K (compared to 354.45 K with water).
- Enhanced Prandtl number with nanofluid coolant (9.74575) compared to water (6.96).
- Overall, the study suggests that a 5% volume fraction of nanofluid yields the most favorable results for enhanced efficiency in the PV/T flat-plate collector system.

### References:

- [1] Tobnaghi, D. M, Madatov, R. and Farhadi, P. 2013. Investigation of light intensity and temperature dependency of solar cells electric parameters. The 2013 Conference on Electric Power Engineering and Control Systems (EPECS-2013), 21- 23 November. LVIV, Ukraine, 90 – 93
- [2] Gielen, D., Boshell, F., Saygin, D., Bazilian, M. D., Wagner, N. and Gorini, R. 2019. The role of renewable energy in the global energy transformation,” *Energy Strategy Reviews*. 24: 38–50.
- [3] Khalil Khanafer, Kambiz Vafai. August 2018. A review on the applications of nanofluids in solar energy field., *Renewable Energy*, Vol. 123, pp. 398-406.
- [4] Prakash, J. 1994. Transient analysis of a photovoltaic-thermal solar collector or co-generation of electricity and hot air/water [Energy Conversion and Management](#). 35: 967-972.
- [5] Lelea D, Calinoiu D.G, Trif-Tordai G, Cioabla A.E, Laza I, Popescu F: The hybrid nanofluid/microchannel cooling solution for concentrated photovoltaic cells. In AIP Conference Proceedings 2015 Feb 17 (1646: 122-128). AIP. DOI: 10.1063/1.4908592
- [6] Al-Waeli A. H, Sopian K, Chaichan MT, Kazem H. A, Hasan H. A, Al-Shamani A. N. 2017. An experimental investigation of SiC nanofluid as a base-fluid for a photovoltaic thermal PV/T system. *Energy Conversion and Management*. 15;142:547-558. DOI: 10.1016/j.enconman.2017.03.076

- [7] Xu Z. and Kleinstreuer C. 2014. Concentration photovoltaic–thermal energy co-generation system using nanofluids for cooling and heating. *Energy Conversion and Management*. 87:504-512. DOI: 10.1016/j.enconman.2014.07.047
- [8] Khanjari, Y., Pourfayaz, F. and Kasaeian, A.B., 2016. Numerical investigation on using of nanofluid in a water-cooled photovoltaic thermal system. *Energy Conversion and Management*, 122: 263-278.
- [9] Chandrasekar, M., Suresh, S., Senthilkumar, T., 2013. Passive cooling of standalone flat PV module with cotton wick structures. *Energy Convers. Manage.* 71: 43–50.
- [10] Soltani S, Kasaeian A, Sarrafha H, Wen D. 2017. An experimental investigation of a hybrid photovoltaic/thermoelectric system with nanofluid application. *Solar Energy*. Oct 1;155:1033-1043. DOI: 10.1016/j.solener.2017.06.069
- [11] Hussien H. A, Noman A. H, and Abdulmunem A. R. 2015. Indoor investigation for improving the hybrid photovoltaic/thermal system performance using nanofluid (Al<sub>2</sub>O<sub>3</sub>-water). *Eng Tech J.* 33:889-901
- [12] Ebaid, M. S., Ghrair, A. M., and Al-Busoul, M. 2018. Experimental investigation of cooling photovoltaic (PV) panels using (TiO<sub>2</sub>) nanofluid in water-polyethylene glycol mixture and (Al<sub>2</sub>O<sub>3</sub>) nanofluid in water-cetyltrimethylammonium bromide mixture. *Energy Conversion and Management*. 155: 324-343. DOI: 10.1016/j.enconman.2017.10.074
- [13] Sardarabadi M, Passandideh-Fard M, Heris SZ. Experimental investigation of the effects of silica/water nanofluid on PV/T (photovoltaic thermal units). *Energy*. 2014 Mar 1;66:264-272. DOI: 10.1016/j.energy.2014.01.102
- [14] Gangadevi R, Vinayagam B. K, Senthilraja S. 2017. Experimental investigations of hybrid PV/ spiral flow thermal collector system performance using Al<sub>2</sub>O<sub>3</sub>/water nanofluid. In *IOP Conference Series: Materials Science and Engineering 2017 May* (Vol. 197, No. 1, p. 012041). IOP Publishing. DOI: 10.1088/1757-899X/197/1/012041
- [15] Mustafa, W., Othman, M. Y., and Fudholi A. 2017. Numerical investigation for performance study of photovoltaic thermal nanofluid system. *International Journal of Applied Engineering Research*. 12(24): 14596-14602
- [16] Kays, W.M., Crawford, M.E., Weigand, B., 2005. *Convective Heat and Mass Transfer*. McGraw-Hill, New York.
- [17] What is cfd — computational fluid dynamics? [Online]. (Accessed: 01- 12-2021). Available: <https://www.simscale.com/docs/simwiki/cfdcomputational-fluid-dynamics/what-is-cfd-computational-fluid-dynamics/>.
- [18] Azmi, W. H., Sharma, K.V., Sarma, P. K, and Mamat, R. 2010. Influence of certain thermo-physical properties on prandtl number of water based nanofluids. *National Conference in Mechanical Engineering Research and Post-graduate Students*. On 26-27 May 2010, FKM Conference Hall, UMP, Kuantan, Pahang, Malaysia; pp. 502-515.
- [19] Verma, S. K. and Tiwari, A. K. 2015. Progress of nanofluid application in solar collectors: a review. *Energy Conversion and Management*, 100:324–346.
- [20] Hasan, A., McCormack, S., Huang, M., Norton, B., 2010. Evaluation of phase change materials for thermal regulation enhancement of building integrated photovoltaics *Sol. Energy* 84(9): 1601–1612.